Chromatic Dispersion in Fiber-Optic Microwave and Millimeter-Wave Links

U. Gliese, S. Nørskov, and T. N. Nielsen

Abstract— **The influence of chromatic fiber-dispersion on the transmission distance of fiber-optic microwave and millimeter-wave links is analyzed and discussed in this paper. It is shown that dispersion significantly limits the transmission distance in intensity modulated direct detection links operating in the above 20 GHz frequency region by inducing a carrier to noise penalty on the transmitted signal. At 60 GHz, a 1 dB penalty is induced after less than 500 m transmission over standard single-mode fiber with a dispersion of 17 ps/km · nm and the signal is completely extinct after 1 km. In remote heterodyne detection links, the dispersion induces both a carrier to noise penalty and a phase noise increase on the transmitted signal. It is shown, however, that the induced carrier to noise penalty is insignificant. At 60 GHz, the induced penalty is less than 0.3 dB after 100 km transmission. The phase noise increase proves more dominant. At 60 GHz, a 150 Mbit/s QPSK signal is limited to around 10 km of transmission.**

I. Introduction

FIBER-OPTIC microwave and millimeter-wave (MW) links, which are subject to a still increasing interest, can be implemented either by the use of direct detection (DD) techniques or remote heterodyne detection (RHD) techniques.[1] Many such links have been proposed, analyzed, and experimented. In the DD-links, the MW-signal is intensity modulated onto the optical carrier from a laser. The optical signal is then transmitted through the optical fiber, and the MW-signal is recovered by DD in a photo-diode. In the RHD-links, two phase correlated optical carriers are generated, in a dual-frequency laser transmitter, with a frequency offset equal to the desired MW-frequency. Further, one of the optical carriers is modulated by the information to be contained in the MW-signal. Both optical signals are then transmitted through the optical fiber, and the MW-signal is generated by heterodyning of the two optical signals in a photo-diode. In both approaches the chromatic fiber-dispersion becomes a limiting factor for the transmission distance when the microwave signals are in the above 20 GHz regime.

The effect of chromatic dispersion is well described for both DD and coherent optical communication systems for transmission of digital baseband signals (see [1], [2] and references herein). It has, however, not yet been fully treated for neither DD nor RHD fiber-optic MW-links. In the DD-links, the dispersion results in a carrier to noise (C/N) penalty on the MW-signal due to phase distortion of the modulation side bands relative to the carrier of the optical signal. In the RHD-links, it results in a C/N penalty as well as an increase of the phase noise on the MW-signal, both due to decorrelation of the two transmitted optical carriers. Further, the two optical carriers often propagate separate paths in the dual-frequency laser transmitter of RHD-links before they are injected into the same fiber. This also introduces signal decorrelation if the paths are not perfectly balanced. The C/N penalty in RHD-links has been treated previously [3], but the dispersion induced phase noise has not yet been investigated.

In this paper we analyze and discuss the dispersion induced C/N penalty for DD-links as well as the dispersion induced C/N penalty and phase noise for RHD-links. Further, we analyze and discuss the influence of path imbalance in the dual-frequency laser transmitters of RHD-links.

The paper is organized as follows: after this introduction, the principle of fiber-optic MW-links based on DD and the influence of chromatic dispersion in these types of links are described in Section II. The same aspects are described in Section III for links based on RHD together with the influence of transmitter path-imbalance. Finally, conclusions are drawn in Section IV.

II. Direct Detection Links

Chromatic fiber-dispersion has a significant influence on the obtainable transmission distance in intensity modulated direct detection (IM-DD) fiber-optic MW-links where the MW-signal (or signal set) is in the above 20 GHz range. The principle of such links is shown in Fig. 1, where $x_{\mathrm{in}}(t)$ is the input MW-signal that is subcarrier modulated onto the optical carrier by electro-optic (E/O) intensity modulation. The resulting optical signal, $y_{\mathrm{in}}(t)$, is transmitted through the fiber to the receiver end. Here, the MW-signal is recovered from the transmitted optical signal, $y_{\mathrm{out}}(t)$, by opto-electric (O/E) direct detection, resulting in the signal $x_{\mathrm{out}}(t)$ that ideally equals the input signal $x_{\mathrm{in}}(t)$. However, due to loss, nonlinearities in the E/O-O/E process and fiber-dispersion, this is not the case. The influence of the chromatic fiber-dispersion is described in the following.

In an IM-DD link, the MW-signal is carried as a lower and an upper side band on the optical carrier. Due to the dispersion and the large frequency offset between the side bands and the optical carrier, the phase of each of the spectral components

Manuscript received January 11, 1996; revised June 14, 1996. This work was supported in part under ESA, ESTEC Contract 134212.

U. Gliese and S. Nørskov are with the Center for Broadband Telecommunications, Department of Electromagnetic Systems, Technical University of Denmark, DK-2800 Lyngby, Denmark.

T. N. Nielsen was with the Center for Broadband Telecommunications, Department of Electromagnetic Systems, Technical University of Denmark, DK-2800 Lyngby, Denmark. He is now with Lucent Technologies Bell Labs Innovations, Murray Hill, NJ USA.

Publisher Item Identifier S 0018-9480(96)06908-6.

[1] Conventional heterodyne detection proves difficult unless lasers with very low phase noise are employed.

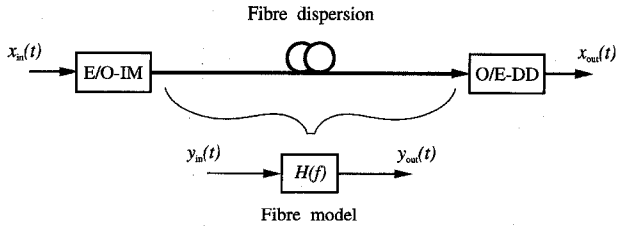

Fig. 1. Principle of intensity modulated direct detection fiber-optic MW-links.

of the transmitted optical signal, $y_{\text{out}}(t)$, has experienced a differential change. After detection, this results in a power reduction of the recovered MW-signal, $x_{\text{out}}(t)$, and thereby a decrease of its carrier to noise ratio (C/N).

To evaluate the dispersion induced C/N penalty, the fiber is modeled as a band-pass filter, cf. Fig. 1, with flat amplitude response and linear group delay. It can be shown that the low-pass equivalent transfer function of the fiber is given by [1]

$$H(f) = \exp^{-j\phi(f)} = \exp^{-j\alpha f^2} \tag{1}$$

where

$$\alpha = \pi D \frac{\lambda^2}{c} L \tag{2}$$

and f is the offset frequency from the optical carrier. Further, D is the chromatic dispersion, λ is the optical wavelength, c is the speed of light in vacuum and L is the length of the fiber. The optical signal at the output of the fiber, $y_{\text{out}}(t)$, is then given by

$$Y_{\text{out}}(f) = Y_{\text{in}}(f)H(f) \tag{3}$$

where $Y_{\text{out}}(f)$ and $Y_{\text{in}}(f)$ are the Fourier transforms of $y_{\text{out}}(t)$ and $y_{\text{in}}(t)$, respectively, given by

$$Y_{\text{out}}(f) = \int_{-\infty}^{\infty} y_{\text{out}}(t)\exp^{-j2\pi ft}dt \tag{4}$$

$$Y_{\text{in}}(f) = \int_{-\infty}^{\infty} y_{\text{in}}(t)\exp^{-j2\pi ft}dt. \tag{5}$$

In the receiver, the MW-signal is recovered by square law detection of the optical signal and is thus given by

$$x_{\text{out}}(t) = |y_{\text{out}}(t)|^2 \tag{6}$$

with a spectrum given by

$$X_{\text{out}}(f) = \int_{-\infty}^{\infty} x_{\text{out}}(t)\exp^{-j2\pi ft}dt. \tag{7}$$

The dispersion induced C/N penalty, on the recovered MW-signal with the carrier frequency f_c, is found by comparing the signal power of $X_{\text{out}}(f_c)$ with and without fiber transmission, respectively

$$\text{Penalty}_{\text{C/N}} = 10\log\left|\frac{X_{\text{out}}(f_{c)\text{ no fiber}}}{X_{\text{out}}(f_c)_{\text{fiber}}}\right|^2. \tag{8}$$

In this paper, the dispersion induced C/N penalty is investigated for an unmodulated MW-carrier given as

$$x_{\text{in}}(t) = \sin(2\pi f_c t) \tag{9}$$

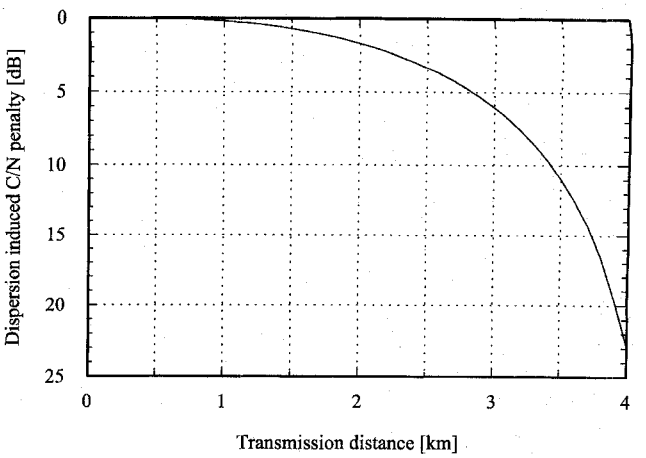

Fig. 2. Dispersion induced C/N penalty as a function of transmission distance for a wavelength of 1550 nm, a chromatic fiber-dispersion of 17 ps/km · nm and a carrier frequency of 30 GHz.

where f_c is the frequency of the MW-carrier. The optical carrier is IM by this input signal resulting in an optical signal with the electrical field of

$$y_{\text{in}}(t) = \sqrt{1+\sin(2\pi f_c t)}\exp^{j2\pi f_{\text{opt}}t} \tag{10}$$

where f_{opt} is the frequency of the optical carrier.

As shown in Fig. 2, for a MW-carrier of 30 GHz, the dispersion results in a significant decrease of the C/N as the transmission distance is increased. This severely limits the obtainable transmission distance in IM-DD fiber-optic MW-links. A complete extinction of the recovered MW-carrier occurs when the phases of the lower and upper side band are π out of phase. This is the case when the phase, αf^2, of $H(f)$ given by (1) has introduced a change of $\pi/2$ on each side band relative to the optical carrier. The transmission distance at which the first complete extinction occurs is found from (2) as

$$L_1 = \frac{c}{2D\lambda^2 f_c^2} \quad \text{for } \alpha f_c^2 = \frac{\pi}{2}. \tag{11}$$

For a MW-carrier at 30 GHz transmitted on an optical carrier at a wavelength of 1550 nm over a standard single-mode fiber with a chromatic dispersion of 17 ps/km · nm, this occurs for a transmission distance of 4.08 km. Further, from Fig. 3, it is seen that the dispersion effect exhibits a cyclic behavior. The period length is found from (2) as

$$\Delta L = \frac{c}{D\lambda^2 f_c^2} \quad \text{for } \alpha f_c^2 = \pi. \tag{12}$$

The periodicity can, as an example, be used to measure chromatic fiber-dispersion in a simple manner but with good accuracy [4].

The amount of dispersion induced C/N penalty that is tolerable in any given link naturally depends on the required link budget and the available margin in each specific case. To generalize the transmission distance investigation, however, a dispersion induced C/N penalty of 1 dB is chosen as acceptable. This value ensures a minimal influence of the dispersion on the entire system performance in terms of C/N.

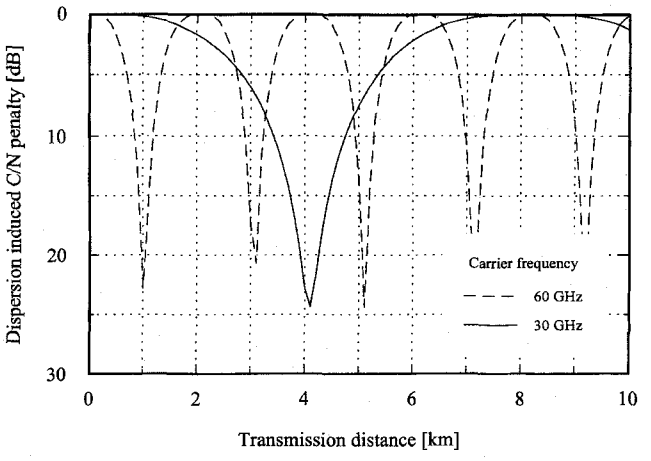

Fig. 3. Dispersion induced C/N penalty as a function of transmission distance for a wavelength of 1550 nm and a chromatic fiber-dispersion of 17 ps/km · nm and with the carrier frequency as parameter.

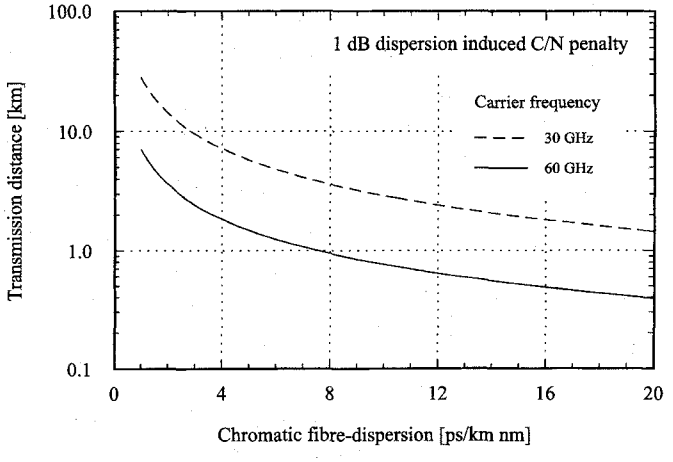

Fig. 4. Obtainable transmission distance as a function of chromatic fiber-dispersion at a wavelength of 1550 nm for a 1 dB dispersion induced C/N penalty and with the carrier frequency as parameter.

The dependance of transmission distance on chromatic fiber-dispersion and MW-carrier frequency is shown in Fig. 4 and Fig. 5, respectively. It is seen that the distance has a $1/D$ dependance on dispersion and a $1/f_c^2$ dependance on carrier frequency. An increase in either dispersion or carrier frequency, therefore, significantly limits the obtainable transmission distance.

It is also seen that the performance can be drastically increased by the use of dispersion shifted fibers. However, for low dispersion values, the tolerance placed on the dispersion is very stringent as a change of a few ps/km nm easily results in a halving of the transmission distance. Although, the dispersion of the fiber is not likely to change significantly, the relative change in dispersion will increase as the dispersion of the fiber decreases. Therefore, in systems applying dispersion shifted fibers this aspect must be carefully considered.

III. Remote Heterodyne Detection Links

All fiber-optic MW-links using RHD are based on the fiber-optic transmission of two phase-correlated optical signals, at

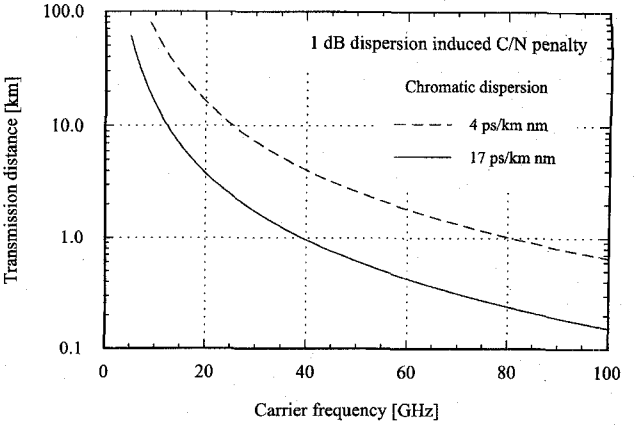

Fig. 5. Obtainable transmission distance as a function of carrier frequency at a wavelength of 1550 nm for a 1 dB dispersion induced C/N penalty and with the chromatic fiber-dispersion as parameter.

frequencies f_1 and f_2, that are offset by the desired MW-carrier frequency f_c. The dual-frequency laser transmitters that are required in these links can be implemented in various ways. A number of different concepts have been proposed and investigated for the fiber-optic transmission and distribution of MW-signals.

1) Dual mode lasers where the two optical signals are generated from two different oscillation modes in a master laser [5].
2) Optical frequency shifting where the two optical signals are generated by:
   —splitting a master laser signal in two and frequency shifting one part [6], [7];
   —single side-band (SSB) modulation of a master laser signal [8], [9];
   —suppressed carrier double side-band (DSB) modulation of a master laser signal [10], [11].
3) Optical offset injection locking where the two optical signals are generated by injection locking of:
   —two slave lasers by a master laser [12];
   —one slave laser by a master laser [13].
4) Optical offset phase locking where the two optical signals are generated by phase locking of a slave laser to a master laser [14]–[21].

A general schematic of the RHD-principle is shown in Fig. 6. With all of the above transmitter concepts, both of the phase-correlated optical signals are phase-equal with the signal from the master laser. For a perfect transmission without influence of the fiber or other optical devices, the two optical signals are also phase-correlated at the remote O/E-detector (photo-diode) where the heterodyning takes place. Consequently, the resulting beat signal is a highly pure MW-carrier at f_c.

However, due to chromatic fiber-dispersion, the two optical signals experience a differential propagation delay, $\Delta\tau_{\text{disp}}$, as they travel the fiber. Furthermore, if the two optical signals, before they are injected into the same fiber, propagate separate paths that are not perfectly balanced, they also experience a differential propagation delay, $\Delta\tau_{\text{path}}$. The sum differential

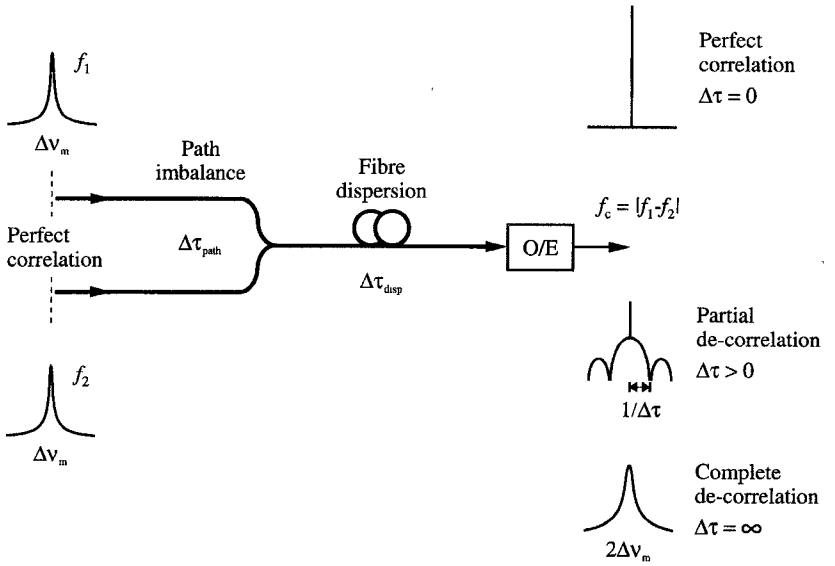

Fig. 6. Principle of remote heterodyne detection fiber-optic MW-links.

propagation delay, given by

$$\Delta\tau = |\Delta\tau_{\text{disp}} + \Delta\tau_{\text{path}}| \tag{13}$$

results in a state of partial phase decorrelation. The amount of decorrelation, and thus the increase in phase noise on the remotely generated MW-carrier, depends, as illustrated in Fig. 6, on the introduced amount of differential delay.

Assuming that the master laser, from which the two phase-correlated optical signals are derived, in the dual-frequency laser transmitter of the link, has a Lorentzian shaped power spectrum, the SSB power spectral density of the MW-signal at the output of the O/E-detector of Fig. 6 is given by [22], [23]

$$\begin{aligned} S(f) = {} & \delta(f)\exp(-2\pi\Delta\nu_{\text{m}}\Delta\tau) \\ & + \frac{\Delta\nu_{\text{m}}}{\pi\{(\Delta\nu_{\text{m}})^2 + f^2\}} \\ & \cdot \Bigg[1 - \exp(-2\pi\Delta\nu_{\text{m}}\Delta\tau) \\ & \cdot \left\{\cos(2\pi f\Delta\tau) + \frac{\Delta\nu_{\text{m}}}{f}\sin(2\pi f\Delta\tau)\right\}\Bigg] \end{aligned} \tag{14}$$

where f is the offset from the MW-carrier and $\Delta\nu_{\text{m}}$ is the full width half maximum (FWHM) linewidth of the power spectrum of the master laser signal. For a small differential delay ($\Delta\tau \simeq 0$), the two optical signals remain correlated and the resulting beat spectrum is a delta function, as illustrated in Fig. 6, given by the first term of (14). At the other extreme, for a very large differential delay, the two optical signals get completely decorrelated. The beat spectrum then becomes Lorentzian shaped given by the second term of (14) and with a linewidth of $2 \cdot \Delta\nu_{\text{m}}$. At intermediate values of $\Delta\tau$, the beat spectrum is a combination of a delta function and a sinc shaped spectrum with spectral zeros spaced by $1/\Delta\tau$.

As seen from (14), the decorrelation results in both a decrease of the C/N (first term) and an increase of the phase noise (second term). These two effects are closely related as the decrease in signal power (and thereby C/N) is due to the increase of phase noise power at all offset frequencies. Both effects must, however, be considered and treated separately, as they may both result in limitations on the allowable differential delay or, in other words, on the obtainable transmission distance.

The delay induced C/N penalty is found from the first term of (14) as

$$\text{Penalty}_{\text{C/N}} = 10\log\left(\frac{1}{\exp^{-2\pi\Delta\nu_{\text{m}}\Delta\tau}}\right). \tag{15}$$

As seen from Fig. 7, where the delay induced C/N penalty is shown as a function of the differential delay with the master laser linewidth as parameter, only a small C/N penalty is induced even for large differential delays and wide master laser linewidths.

The phase noise of the MW beat signal is best investigated by considering the phase fluctuation spectrum, $S_\phi(f)$, rather than the power spectrum of (14). From the above, it is clear that the delay introduces differential phase fluctuations on the MW-signal. These are expressed from the master laser frequency fluctuation spectrum, $S_{\text{f}}(f)_{\text{m}}$, as [24]

$$S_\phi(f)_{\text{delay}} = 2 \cdot \frac{S_{\text{f}}(f)_{\text{m}}}{f^2} \cdot \{1 - \cos(2\pi f\Delta\tau)\}. \tag{16}$$

If the master laser has a Lorentzian power spectral shape, then (16) simplifies to

$$S_\phi(f)_{\text{delay}} = \frac{2\Delta\nu_{\text{m}}}{\pi f^2} \cdot \{1 - \cos(2\pi f\Delta\tau)\}. \tag{17}$$

This spectrum is shown in Fig. 8 as a function of frequency off the carrier with the differential delay as parameter. The $1/f^2$ shape resulting from the Lorentzian power spectral shape

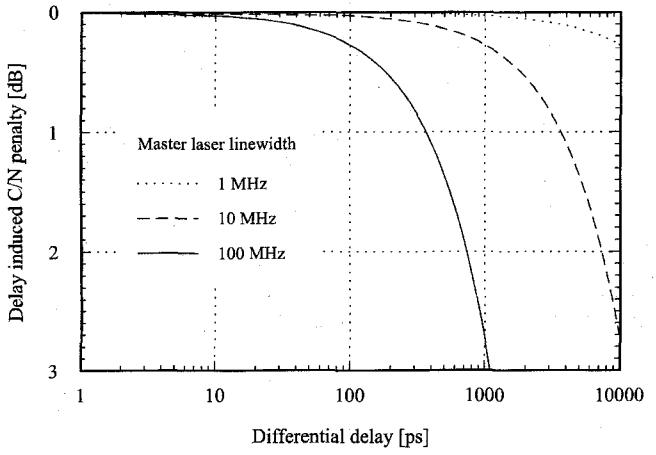

Fig. 7. Delay induced C/N penalty as a function of differential delay with the master laser linewidth as parameter.

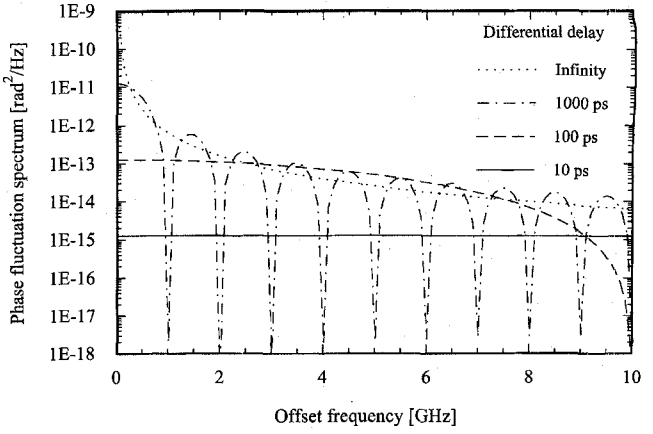

Fig. 8. Phase fluctuation spectral density of the remote heterodyne beat signal with the differential delay as parameter for a master laser linewidth of 1 MHz.

is clearly identified for an infinite differential delay. Further, the sinc shape is clearly seen for intermediate values of the differential delay. Finally, for values in the range below a few hundreds of pico seconds, it is seen that the distribution of the phase noise versus frequency is quite uniform due to the long distance between spectral zeros of the sinc. This indicates that, a significant amount of the delay induced phase noise will be removed by the filtering performed in any MW-receiver [16]. Therefore, this filtering must be taken into account when calculating the exact amount of delay induced phase noise.

The phase noise is expressed as rms phase error σ_ϕ or as phase variance $(\sigma_\phi)^2$ given by

$$(\sigma_\phi)^2_{\text{delay}} = \int_0^{B_n} \frac{2\Delta\nu_m}{\pi f^2} \cdot \{1 - \cos(2\pi f \Delta\tau)\} df \simeq 2\pi\Delta\nu_m B_n (\Delta\tau)^2 \quad \text{for } B_n \ll \frac{1}{\Delta\tau} \tag{18}$$

where B_n is the MW-receiver noise bandwidth. As shown in Fig. 9, the delay induced rms phase error has been calculated from (18) as a function of the differential delay with the master laser linewidth times the receiver noise bandwidth as parameter. It is seen that the delay induced rms phase error increases as the differential delay increases. Further, an increase in either master laser linewidth or receiver noise bandwidth also cause an increase of the rms phase error.

The first part of the differential delay in (13) is due to chromatic fiber-dispersion and depends on the transmission distance, L, the wavelength λ, the frequency offset, f_c (the MW-carrier frequency), between the two optical signals and the fiber-dispersion, D. This part constitutes the delay reference and is therefore always taken as positive. It is given by

$$\Delta\tau_{\text{disp}} = D \cdot L \cdot \frac{\lambda^2}{c} \cdot f_c. \tag{19}$$

The other part, the path imbalance delay, is present, if the two optical signals at any time propagate different paths. This is often the case in the transmitter of RHD-links. The delay due to difference in path length is given by

$$\Delta\tau_{\text{path}} = \pm\frac{\Delta L_{\text{path}} \cdot n}{c} \tag{20}$$

where ΔL_{path} is the difference in path length and n is the refractive index of the device material. The sign of the path imbalance delay depends on whether it works in the same or the opposite direction as the dispersion induced delay. This naturally depends on how the two optical signals, at frequencies f_1 and f_2, are delayed to one another by the path imbalance in relation to how they are delayed to one another by the dispersion.

The sum differential delay, (13), is shown in Fig. 10 as a function of the transmission distance times the MW-carrier frequency with the path imbalance delay as parameter for a wavelength of 1550 nm and a chromatic fiber-dispersion of 17 ps/km·nm. Results for other values of the dispersion are easily read from the curves as well, because the delay and the dispersion have a one to one dependency. It is seen that the delay increases with both distance and carrier frequency. Obviously, dispersion shifted fibers can be used to reduce the dispersion induced delay and thereby the dispersion induced rms phase error. Further, it is seen, that a positive path imbalance delay contributes a delay floor equal to its value. In contrast, a negative path imbalance delay brings the sum differential delay to zero for one distinct combination of transmission distance and carrier frequency. Consequently the path imbalance delay can be used to compensate the dispersion induced delay for a fixed distance times carrier frequency product.

The total delay induced rms phase error on the MW-carrier, after receiver filtering, is found from a knowledge of transmission distance, carrier frequency, wavelength, dispersion, path imbalance delay, master laser linewidth and receiver bandwidth by use of Figs. 9 and 10.

To investigate the influence of the delay induced rms phase error it is necessary to know the allowable rms phase error in the different types of MW-systems for which the signals are to be transmitted over the fiber-optic link. This is investigated for M-ary PSK MW-systems by calculating the rms phase errors that introduces a 1 dB sensitivity penalty at a 10^{-9} bit error rate (BER) using the formulas of Appendix A. The results of these calculations are listed in Table I. Most often,

TABLE I
THE ALLOWABLE RMS PHASE ERROR FOR DIFFERENT TYPES OF MICROWAVE SYSTEMS

Type of system	Allowable rms phase error		
	1 dB penalty at a 10^{-9} BER	Typical	10% of typical
PSK	11.4°	8.2°	0.82°
QPSK	3.9°	2.8°	0.28°
8PSK	1.8°	1.3°	0.13°
16PSK	1.2°	0.9°	0.09°

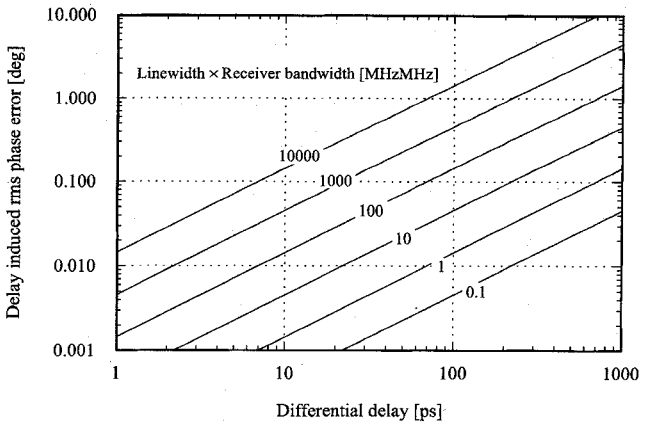

Fig. 9. Delay induced rms phase error as a function of the differential delay with the master laser linewidth times the receiver noise bandwidth as parameter.

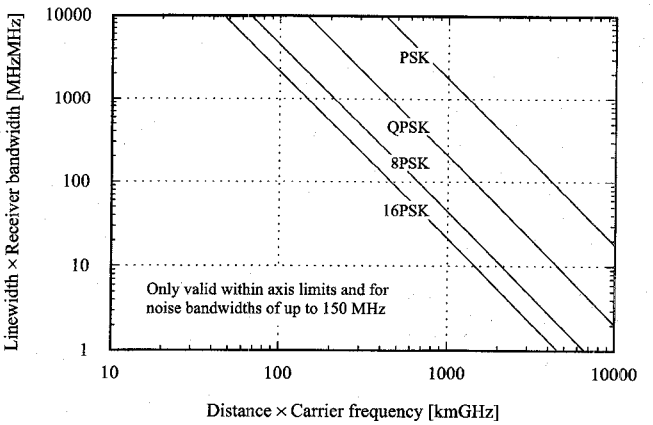

Fig. 11. The masterlaser linewidth times the receiver noise bandwidth as a function of the transmission distance times carrier frequency for different types of systems, and for a wavelength of 1550 nm and a chromatic fiber dispersion of 17 ps/km · nm.

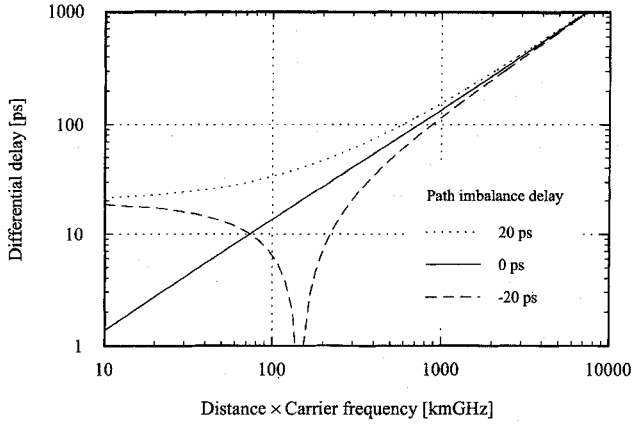

Fig. 10. Differential delay as a function of transmission distance times the MW-frequency with the path imbalance delay as parameter for a wavelength of 1550 nm and a chromatic fiber dispersion of 17 ps/km · nm.

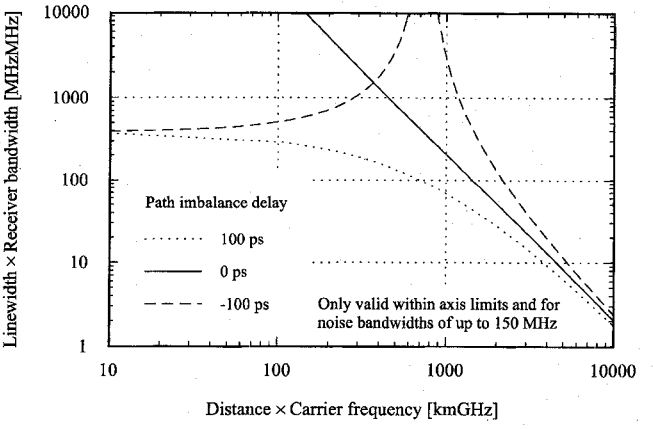

Fig. 12. The masterlaser linewidth times the receiver noise bandwidth as a function of the transmission distance times carrier frequency for a QPSK system with the path imbalance delay as parameter for a wavelength of 1550 nm and a chromatic fiber dispersion of 17 ps/km · nm.

however, the total allowable rms phase errors are somewhat lower. Therefore, the total rms phase errors, that are typically allowed in standard MW-receivers are shown as well. The typical values are based on the Intelsat specifications for a QPSK system, allowing maximum 2.8° [25]. The values for PSK, 8PSK, and 16PSK are extrapolated from this value using the ratios between the values for the 1 dB penalty case. As the values allowed in standard systems are maximum values incorporating all phase noise sources, the acceptable delay induced rms phase error should only constitute a fraction of these. In this paper, an acceptable value is chosen as 10% of the values required in standard MW-systems.

As seen from (18), the delay induced rms phase error depends on the master laser linewidth, the MW-receiver noise bandwidth and the sum differential delay, (13). The latter is composed of a dispersion induced delay, (19), that depends on the transmission distance and the MW carrier frequency, and a path imbalance delay, (20). Based on the 10% values of Table I, the master laser linewidth times the MW-receiver noise bandwidth is shown as a function of the transmission distance times carrier frequency product in Fig. 11. It is seen that the obtainable transmission distance times carrier frequency product decreases as the master laser linewidth

or the MW-receiver noise bandwidth increases. The curves are used to determine the obtainable transmission distance times carrier frequency for a given master laser linewidth and MW-receiver noise bandwidth of different systems. If, as an example, a 150 Mbit/s QPSK MW-signal, which has a single sided noise bandwidth of 45 MHz [25], is transmitted over a RHD fiber-optic link using a master laser with a linewidth of 10 MHz, then the obtainable distance times carrier frequency product is 640 km · GHz, e.g., a transmission distance of approximately 10 km for a carrier frequency of 60 GHz. The distance is increased to approximately 30 km by reducing the master laser linewidth to 1 MHz. In both cases it is found from Fig. 7 that the delay induced C/N penalty is well below a tenth of a dB.

From the above, it is seen that, even for wide bandwidth systems at high carrier frequencies, it is possible to transmit over long fiber-distances with RHD-links using master lasers with linewidths in the 1–10 MHz range.

As shown in Fig. 12 for a QPSK system, the situation can be improved or worsened by the presence of a path imbalance delay depending on whether it counteracts (negative path imbalance delay) the dispersion induced delay or not, respectively. For small values of the distance times carrier frequency product, the dispersion induced delay is close to zero. A negative or positive path imbalance delay therefore limits the linewidth times receiver bandwidth product. As the distance times carrier frequency product increases, the absolute value of the positive dispersion induced delay increases toward the absolute value of the negative path imbalance delay. This eventually results in a sum differential delay of zero at a given distance times carrier frequency product. At this point there is, consequently, no limit on the linewidth times MW-receiver bandwidth product. When the dispersion induced delay increases further, the sum delay begins to increase, and the linewidth or the MW-receiver bandwidth has to be reduced. A negative path imbalance delay can thus be applied, in the transmitter of RHD-links, to reduce the dispersion induced rms phase error around a fixed distance times carrier frequency product. In this case, however, the rms phase error will increase if the product is lowered.

IV. Conclusion

In this paper we have shown that chromatic fiber-dispersion puts a limit on the obtainable transmission distance in both IM-DD and RHD fiber-optic MW-links.

In the DD-links, the dispersion results in a carrier to noise (C/N) penalty on the MW-signal due to phase distortion of the modulation side bands relative to the carrier of the optical signal. This effect is independent of the modulation format of the MW-signal as well as on the laser linewidth, and, therefore apply equally for any type of MW-signal. For links operating above 20 GHz, the dispersion induced C/N penalty becomes significant even after short transmission distances. At 60 GHz, a 1 dB penalty is induced after 500 m transmission over standard single-mode fiber with a dispersion of 17 ps/km · nm and the signal is completely extinct after 1 km. Reducing the dispersion improves the situation on a one to one scale. However, as the dispersion is reduced, the induced penalty becomes more sensitive to fluctuations in dispersion as the relative change in dispersion will increase as the dispersion of the fiber decreases. In systems applying dispersion shifted fibers, this aspect must be carefully considered.

In the RHD-links, the dispersion results in a C/N penalty as well as an increase of the phase noise on the MW-signal, both due to decorrelation of the two transmitted optical carriers. The C/N penalty effect is, as in the direct link, independent of the modulation format of the MW-signal, and, therefore also apply equally for any type of MW-signal. The effect, however, is dependant on the master laser linewidth. It has been shown that the induced carrier to noise penalty is insignificant. At 60 GHz, the induced penalty is less than 0.3 dB after 100 km transmission over standard single-mode fiber with a dispersion of 17 ps/km · nm even for a master laser linewidth as wide as 10 MHz.

The phase noise increase proves much more dominant. At 60 GHz, a 150 Mbit/s QPSK signal is limited to around 10 km of transmission over standard single-mode fiber with a dispersion of 17 ps/km·nm for a master laser linewidth of 10 MHz. A tenfold reduction of the linewidth to 1 MHz allows for a threefold increase in transmission distance to 30 km. In general M-ary PSK signals with a low value of M are less affected and those with a high value of M are more affected. With a laser linewidth of 10 MHz, a 150 Mbit/s PSK signal at 60 GHz is limited to 20 km, and a 150 Mbit/s 16PSK signal is limited to 5 km. Still the limitation is far less significant than for DD-links, and it is seen that it is possible to transmit over quite long distances with RHD-links using master lasers with linewidths in the 1–10 MHz range. Further, the dispersion induced phase noise can be reduced if the two optical signals, in the transmitter, propagate separate paths with a path imbalance delay that counteracts the dispersion induced delay. It must, however, be noted that the reduction only applies around a fixed value of transmission distance times carrier frequency. Great care must, therefore, be exercised in designing the dual-frequency laser transmitters of RHD-links.

In conclusion, both direct detection and remote heterodyne detection fiber-optic microwave and millimeter-wave links are limited in transmission distance by chromatic fiber-dispersion when operating in the above 20 GHz range. The effect in DD-links is severe whereas it is tolerable in RHD-links. Further, in RHD-links, the dispersion effect can be compensated by the use of separated signal paths in the transmitters of the links.

Appendix A
BER in M-ary PSK Microwave Systems

In this Appendix we give equations for the bit error rate (BER) in M-ary PSK MW-systems. The equations take into account the phase noise as well as the additive noise.

A symbol decision error is made in the receiver of the system if noise-additive Gaussian noise and carrier phase noise-causes the phase of the received symbol to fall outside the range $-\pi/M \leq \phi \leq \pi/M$ relative to its ideal value. By weighing the magnitude of the mean phase error by its

probability we obtain the symbol error probability

$$P_{\text{sym}} = 1 - \sum_{k=0}^{M-1} P_k \int_{-\pi/M}^{+\pi/M} p(\phi). \tag{21}$$

The interval between two nearby phase states for an M-ary PSK signal equals $\Delta\phi = 2\pi/M$. It is easily seen, that the probability of a phase change of $k \cdot \Delta\phi$ during a symbol transition is given by

$$\begin{aligned} P_{k\cdot\Delta\phi|_{k=0}} &= \frac{1}{M}, \\ P_{k\cdot\Delta\phi|_{k\neq 0}} &= \frac{2(M-k)}{M^2}. \end{aligned} \tag{22}$$

The pdf of ϕ depends on the additive noise as well as the residual phase noise of the optically generated MW-carrier. The pdf of ϕ for the additive Gaussian noise is given by [26]

$$p_1(\phi) = \frac{\exp^{-\gamma}}{2\pi}\left(1 + \sqrt{2\gamma}\cos\phi \cdot \exp^{\gamma\cos^2\phi} \cdot \int_{-\infty}^{\sqrt{2\gamma}\cos\phi} \exp^{-x^2/2}\, dx\right) \tag{23}$$

where γ is the carrier to noise ratio (C/N) of the M-ary PSK carrier signal.

For simplicity we assume the phase noise to have a Gaussian pdf given by

$$p_2(\phi) = \frac{1}{\sigma_\phi\sqrt{2\pi}} \exp^{-\frac{\phi^2}{2\sigma_\phi^2}} \tag{24}$$

where σ_ϕ is the rms phase error. Since $p_1(\phi)$ and $p_2(\phi)$ are independent random processes their joint pdf, $p(\phi)$ is given by their convolution

$$p(\phi) = \int_{-\pi}^{+\pi} p_1(x)p_2(\phi - x)dx. \tag{25}$$

Assuming that a Gray code is used for the symbol mapping and that the noise is sufficiently low so that a symbol error only results in a single bit error we obtain the bit error rate by

$$\text{BER} = \frac{P_{\text{sym}}}{\log_2(M)}. \tag{26}$$

ACKNOWLEDGMENT

The authors would like to thank R. Hoffstetter of Alcatel SEL, A. Seeds of University College London, N. Vodjdani of Thomson CSF, D. Wake of British Telecom and other participants at the 1994 IEEE Topical Meeting on Optical Microwave Interactions for fruitful discussions during the meeting. Further, we thank K. E. Stubkjær and R. J. Pedersen of the Technical University of Denmark for fruitful discussions.

REFERENCES

[1] A. F. Elrefaie, R. E. Wagner, D. A. Atlas, and D. G. Daut, "Chromatic dispersion limitations in coherent lightwave transmission systems," *IEEE J. Lightwave Technol.*, vol. 6, no. 5, pp. 704–709, 1988.

[2] A. F. Elrefaie and R. E. Wagner, "Chromatic dispersion limitations for FSK and DPSK systems with direct detection receivers," *IEEE Photon. Technology Lett.*, vol. 3, no. 1, pp. 71–73, 1991.

[3] R. Hofstetter, H. Schmuck, and R. Heidemann, "Dispersion effects in optical millimeter-wave systems using self-heterodyne method for transport and generation," *IEEE Trans. Microwave Theory Tech.*, vol. 43, no. 9, pp. 2263–2269, 1995.

[4] F. Devaux, Y. Sorel, and J. F. Kerdiles, "Simple measurement of fiber dispersion and of chirp parameter of intensity modulated light emitter," *IEEE J. Lightwave Technol.*, vol. 11, no. 12, pp. 1937–1940, 1993.

[5] D. Wake, C. R. Lima, and P. A. Davies, "Optical generation of millimeter-wave signals for fiber-radio systems using a dual mode DFB semiconductor laser," *IEEE Trans. Microwave Theory Tech.*, vol. 43, no. 9, pp. 2270–2276, 1995.

[6] M. Tamburrini, M. Parent, L. Goldberg, and D. Stillwell, "Optical feed for a phased array microwave antenna," *IEE Electron. Lett.*, vol. 23, no. 13, pp. 680–681, 1987.

[7] C. L. Wang, Y. Pu, and C. S. Tsai, "Permanent magnet-based guided-wave magnetooptic Bragg cell modules," *IEEE J. Lightwave Technol.*, vol. 10, no. 5, pp. 644–648, 1992.

[8] M. Izutsu, S. Shikama, and T. Sueta, "Integrated optical SSB modulator/frequency shifter," *IEEE J. Quantum Electron.*, vol. QE-17, no. 11, pp. 2225–2227, 1981.

[9] R. A. Soref, "Voltage-controlled optical/RF phase shifter," *IEEE J. Lightwave Technol.*, vol. LT-3, no. 5, pp. 992–998, 1985.

[10] J. J. O'Reilly, P. M. Lane, R. Heidemann, and R. Hofstetter, "Optical generation of very narrow linewidth millimeter wave signals," *IEE Electron. Lett.*, vol. 28, no. 25, pp. 2309–2311, 1992.

[11] H. Schmuck, R. Heidemann, and R. Hofstetter, "Distribution of 60 GHz signals to more than 1000 base stations," *IEE Electron. Lett.*, vol. 30, no. 1, pp. 59–60, 1994.

[12] L. Goldberg, H. F. Taylor, and J. F. Weller, "Microwave signal generation with injection-locked laser diodes," *IEE Electron. Lett.*, vol. 19, no. 13, pp. 491–493, 1983.

[13] L. Goldberg, A. M. Yurek, H. F. Taylor, and J. F. Weller, "35 GHz microwave signal generation with an injection-locked laser diode." *IEE Electron. Lett.*, vol. 21, no. 18, pp. 814–815, 1985.

[14] R. C. Steele, "Optical phase-locked loop using semiconductor laser diodes," *Electron. Lett.*, vol. 19, no. 2, pp. 69–70, 1983.

[15] K. J. Williams, L. Goldberg, R. D. Esman, M. Dagenais, and J. F. Weller, "6–34 GHz offset phase-locking of Nd:YAG 1319 nm nonplanar ring lasers," *IEE Electron. Lett.*, vol. 25, no. 18, pp. 1242–1243, 1989.

[16] U. Gliese, E. L. Christensen, and K. Stubkjær, "Laser linewidth requirements and improvements for coherent optical beam forming networks in satellites," *J. Lightwave Technol.*, vol. 9, no. 6, pp. 779–790, 1991.

[17] R. T. Ramos and A. J. Seeds, "Fast heterodyne optical phase-lock loop using double quantum well laser diodes," *IEE Electron. Lett.*, vol. 28, no. 1, pp. 82–83, 1992.

[18] U. Gliese, T. N. Nielsen, M. Bruun, E. L. Christensen, K. E. Stubkjær, S. Lindgren, and B. Broberg, "A wideband heterodyne optical phase locked loop for generation of 3–18 GHz microwave carriers," *IEEE Photon. Technol. Lett.*, vol. 4, no. 8, pp. 936–938, 1992.

[19] T. N. Nielsen, U. Gliese, J. Riishøj, K. E. Stubkjær, P. Doussiere, P. Grabedian, F. Martin-Leblond, J. L. Lafragette, D. Leclerc, and B. Fernier, "A Gbit/s QPSK optical microwave transmitter based on a semiconductor optical amplifier phase modulator and phase locked DFB lasers," in *Tech. Dig. Conf. Opt. Fiber Communicat.*, San Jose, CA, Feb. 1994, pp. 114–115.

[20] T. N. Nielsen, U. Gliese, K. E. Stubkjær, T. Christensen, and H. Høgh, "Highly linear and transparent 3–18 GHz optical microwave link," in *Tech. Dig. IEEE MTT-S Int. Microwave Symp.*, San Diego, CA, May, 1994, pp. 491–494.

[21] U. Gliese, T. N. Nielsen, S. N. Nielsen, and K. E. Stubkjær, "Frequency up-shifting fiber-optic microwave link," in *Proc. IEEE MTT-S & LEOS Topical Meet. Opt. Microwave Interactions*, Abbaye de Vaux de Cernay, France, Nov. 1994, pp. 137–139.

[22] P. Gallion, F. J. Mendieta, and R. Leconte, "Single-frequency laser phase-noise limitation in single-mode optical-fiber coherent-detection systems with correlated fields," *J. Opt. Soc. America*, vol. 72, no. 9, pp. 1167–1170, 1982.

[23] P. B. Gallion and G. Debarge, "Quantum phase noise and field correlation in single frequency semiconductor laser systems," *IEEE J. Quantum Electron.*, vol. QE-20, no. 4, pp. 343–349, 1984.

[24] H. E. Rowe, *Signals and Noise in Communication Systems*. New York: Van Nostrand, 1965, pp. 113–116.
[25] Intelsat earth station standards (IESS), "QPSK/FDMA performance characteristics for Intelsat business services (IBS)," Document IESS-309 (Rev. 2), Approval date: Mar. 9, 1990, p. 14.
[26] J. G. Proakis, *Digital Communications*. New York: McGraw-Hill, 1989.

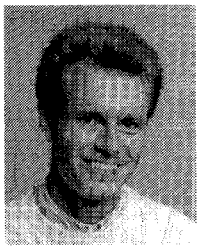

U. Gliese was born in 1965. He received the M.Sc.E.E. and Ph.D. degrees from the Technical University of Denmark (TUD) in 1989 and 1992, respectively.

From 1992 to 1995 he was a Senior Researcher at TUD. He has worked with fiber-optics for microwave applications since 1989 and has been Work Package Manager on several contracts with the European Space Agency. His research activities have covered coherent optical communication systems, microwave devices, characterization of advanced semiconductor lasers, optical phase locked loops for generation of microwave to submillimeter-wave signals, laser phase noise reduction by phase conjugate feedback, optical modulation, opto-electronic MMIC devices and fiber-optic microwave links. Presently, he is Associate Research Professor and is Project Manager for work on Optical Networks for Microwave Communications at the Center for Broadband Telecommunications at TUD.

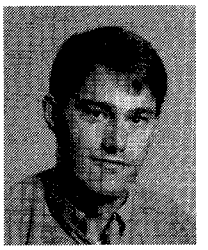

S. Nørskov was born in 1966. He received the M.Sc.E.E. degree from the Technical University of Denmark (TUD) in 1994.

His research activities have covered phase locked loops for clock recovery in 10–20 Gbit/s optical communication systems and ATM traffic modeling. Presently, he is pursuing the Ph.D. degree at TUD working on optical networks and network management for ATM based multimedia mobile communication networks under the project Optical Networks for Microwave Communications at the Center for Broadband Telecommunications at TUD.

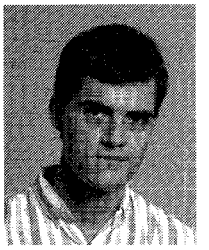

T. N. Nielsen was born in 1965. He received the M.Sc.E.E. and Ph.D. degrees from the Technical University of Denmark (TUD) in 1991 and 1994, respectively.

Dr. Nielsen has worked with fiber-optics for microwave applications since 1991 and has been work package manager on several contracts with the European Space Agency. His research activities have covered broadband microwave amplifiers, modeling and characterization of semiconductor optical amplifiers, optical modulation with semiconductor optical amplifiers, optical phase locked loops for generation of microwave to submillimeter-wave signals, laser phase noise reduction by phase conjugate feedback, opto-electronic MMIC devices and fiber-optic microwave links. Presently, he is Member of Technical Staff at Lucent Technologies Bell Labs Innovations working on analog fiber-optic transmission systems.